

Low thermal conductivity of SnSe and existence of an easy axis for phonons

Jesús Carrete,¹ Natalio Mingo,^{1, a)} and Stefano Curtarolo^{2, b)}

¹⁾CEA-Grenoble, 17 Rue des Martyrs, Grenoble 38054, France

²⁾Center for Materials Genomics, Materials Science, Electrical Engineering, Physics and Chemistry, Duke University, Durham, North Carolina 27708, USA

In this theoretical study, we investigate the origins of the very low thermal conductivity of tin selenide (SnSe) using *ab-initio* calculations. We obtained high-temperature lattice thermal conductivity values that are close to those of amorphous compounds. We also found a strong anisotropy between the three crystallographic axes: one of the in-plane directions stands out as an easy axis for thermal transport. Our results are compatible with most of the experimental literature on SnSe, and differ markedly from the more isotropic values reported by a recent study.

The ongoing quest for improved thermoelectric materials has spanned the past six decades.^{1,2} Good thermoelectrics are characterized by their high figures of merit $ZT = PT/\kappa$. This requires a low thermal conductivity κ , and a high power factor $P = \sigma S^2$ (where σ is the electrical conductivity, and S the thermopower) across their intended range of working temperatures. Nanotechnology has been able to greatly improve on earlier single-crystal thermoelectric materials³ via hindering phonon flow while keeping favorable electric properties, even when starting from a poor performer such as bulk silicon.⁴

Thus, it was somewhat surprising when single-crystal SnSe recently emerged as the best thermoelectric material ever measured. Experimental measurements on monocrystalline samples⁵ point to a record figure of merit of $ZT = 2.6$ at $T = 923$ K. This is due mainly to its very low lattice thermal conductivity κ_ℓ . Intense interest in SnSe was spurred by these results, and to date two independent sets of measurements on polycrystals have been published.^{6,7} The two series are compatible with each other, yet they both display higher values of κ than those reported in Ref. 5 for the single crystal. This contrasts with the expectation that grain boundaries should act as sources of scattering, and decrease the thermal conductivity below that of the single crystal. Remarkably, preexisting studies of single crystals⁸ reported even higher values of κ , with a directional maximum of around $1.8 \text{ W m}^{-1} \text{ K}^{-1}$ at room temperature.

To address this controversy, we studied phonon transport in SnSe from first principles based on the Boltzmann transport equation (BTE) formalism. Such modeling studies offer substantially more detailed information than is readily available from the experiments, and have demonstrated both their wide range of applicability and their predictive power.^{9–13} For the present work, we focused on the Pnma-symmetric phase of SnSe. This is the stable phase from room temperature up to $\sim 750 - 800$ K.⁵ Hence, it is the pertinent phase for most of the aforementioned measurements.^{5–7} At values

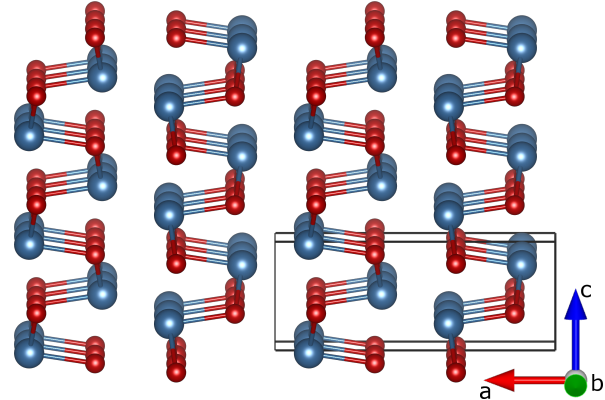


FIG. 1. View of a $2 \times 3 \times 3$ supercell of Pnma SnSe. A grey prism outlines a single unit cell, containing 8 atoms.

above the transition temperature, SnSe adopts a higher-symmetry Cmc m phase.

We started with an atomistic description of Pnma SnSe extracted from the AFLOWLIB.org consortium repository [auid=afLOW:d188eb9b8df60e58].^{14,15} We relaxed the structure without any geometrical constraint using the density functional theory (DFT) software package VASP.¹⁶ This was performed using the local density approximation,¹⁷ along with projector-augmented-wave pseudopotentials.¹⁸ Other relevant parameters include an energy cutoff of 313 eV and a $6 \times 10 \times 10$ Γ -centered mesh in reciprocal space. We obtained unit cell lengths of $a = 11.72 \text{ \AA}$, $b = 4.20 \text{ \AA}$ and $c = 4.55 \text{ \AA}$, which are in reasonable agreement with the literature.^{5,6,19} The relaxed structure is shown in Fig. 1. From a geometric point of view, the b and c axes are almost equivalent, while the a axis is almost triple their length. By virtue of the interatomic distances involved, this phase can be described as quasi-laminar. In the relaxed structure, b and c are the two “in-plane” axes and a is the “cross-plane” axis.

We next computed sets of second- and third-order interatomic force constants using a $3 \times 5 \times 5$ supercell containing 600 atoms. We additionally obtained the dielectric parameters of the system to account for long-range Coulombic interactions: a set of Born effective charges, and the dielectric tensor in the infinite-frequency limit. This information is sufficient for obtaining the phonon

^{a)}Electronic mail: natalio.mingo@cea.fr

^{b)}Electronic mail: stefano@duke.edu

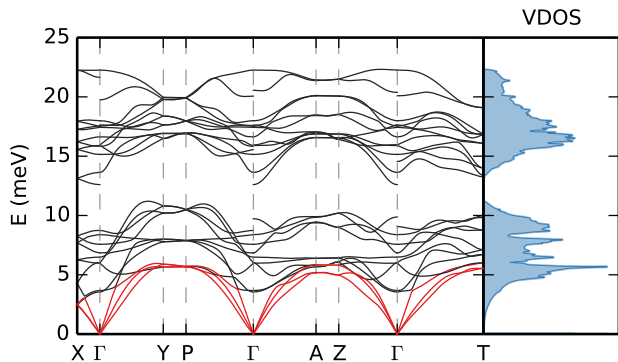


FIG. 2. Phonon dispersion curves and vibrational density of states (VDOS) for the Pnma phase of SnSe. Acoustic modes are highlighted in red.

spectrum and three-phonon scattering rates required to solve the fully linearized BTE. We used the Phonopy package²⁰ for the second-order calculations. To obtain the third-order force constants and to solve the BTE, we employed our own software. All the required forces were obtained from DFT calculations with VASP. Our workflow is documented in full detail elsewhere, and the source code we used in this implementation is publicly available for download under an open source license.²¹

The computed phonon spectrum is shown in Fig. 2. The vibrational density of states has a bipartite structure, with a phononic gap centered at approximately 11.8 meV that delimits two groups, each with twelve branches. The Pnma unit cell of SnSe may be conceptualized as a distorted variation of a simpler diatomic rocksalt structure.⁵ This is consistent with a bipartite spectrum whose lower (upper) half corresponds roughly to the folded acoustic (optical) modes of the rocksalt unit cell. Another conclusion that may be drawn from this line of reasoning is that speeds of sound (slopes of the acoustic modes close to the Γ point) should be roughly isotropic. This is confirmed by direct calculation, and is also apparent in Fig. 2. Nevertheless, the much shorter length of the reciprocal-space unit cell along a^* allows us to anticipate a much lower value of κ_ℓ along a . This lowered value arises from purely geometric considerations.

Our results for single-crystal SnSe, at temperatures from 300 K to 775 K, are plotted and compared with experimental data⁵ in Fig. 3. All values of κ_ℓ are remarkably low for a crystalline material.²²

This is to a large extent a result of the low-frequency spectrum, which in turn is due to the heavy atomic masses. We detected a strong anisotropy between the three axes, with $\kappa_\ell^b > \kappa_\ell^c > \kappa_\ell^a$ at all temperatures. Our computed value of κ_ℓ^a is in rather good agreement with experimental measurements. Intriguingly, our results for the remaining two axes disagree markedly with Ref. 5. The recent experimental results point to an almost isotropic thermal conduction along the bc plane, and an in-plane room-temperature $\kappa_\ell \sim 0.7 \text{ W m}^{-1} \text{ K}^{-1}$.

Instead, we clearly identify b as an easy axis for phonon flow, with a factor-of-two difference in κ_ℓ with respect to c , and an average in-plane $\kappa_\ell \sim 1.4 \text{ W m}^{-1} \text{ K}^{-1}$ at 300 K. Our data are more in line with historical measurements on this system.⁸ The origin of this bc anisotropy can be traced to the phonon dispersions in Fig. 2: the average phonon frequencies and group velocities are higher along $\Gamma \rightarrow Y$ than along $\Gamma \rightarrow Z$. A finer analysis reveals that the source of this in-plane anisotropy are modes in the lower half of the spectrum — in fact, the contribution to κ_ℓ from optical modes above the gap is very similar along both directions.

To test the hypothesis that the frequencies and group velocities of modes below the gap give rise to the anisotropic in-plane conduction, we have studied the tensor quantity:

$$C^{\alpha\beta} = \frac{24k_B}{\Omega} \left[\frac{x}{\sinh(x)} \right]^2 v^\alpha v^\beta, \quad (1)$$

for each branch at each point of the Brillouin zone (BZ). Here, Ω is the unit cell volume, k_B is the Boltzmann constant, x is defined as $(2k_B T)^{-1} \hbar \omega$, ω is an angular frequency and \mathbf{v} a group velocity. The average of $C^{\alpha\beta\tau}$ (where τ^{-1} is the scattering rate) among phonon branches and over the BZ is the lattice thermal conductivity tensor.²¹ Thus, $C^{\alpha\beta}$ accounts for the influence of the phonon spectrum on κ_ℓ . For the phonon branches below the gap in SnSe, C^{bb} is on average two to three times higher than C^{cc} . As scattering rates are substantially higher for the high-frequency modes, it is modes below the gap that contribute the most significantly to κ_ℓ . Hence, the anisotropy of $C^{\alpha\beta}$, determined by frequencies and group velocities alone, is sufficient to explain the difference between κ_ℓ^b and κ_ℓ^c .

As the phonon spectrum is computed from forces caused by small nuclear displacements, the anisotropy of $C^{\alpha\beta}$ must ultimately be due to a mechanical anisotropy of the material. As is illustrated in Fig. 1, despite the similar dimensions of its unit cell along b and c , Pnma SnSe is far from isotropic in the bc plane. Along b , the compound can be considered as a series of zig-zagging SnSe chains, with a Sn-Se distance of 2.82 Å. Along c , a second Sn-Se distance of 3.43 Å must also be considered.

One of the causal factors behind SnSe's ultra-low thermal conductivity is the presence of very long-range interactions that play a crucial role in phonon scattering. We had to use an exceptionally long cutoff radius for anharmonic interactions in our calculations ($\sim 6.5 \text{ nm}$, or the 19th coordination sphere in this low-symmetry structure) to obtain converged values of κ_ℓ . As evidenced by the results shown in Fig. 4, interactions between atoms more than $\sim 6 \text{ nm}$ apart are responsible for a $\sim 40\%$ drop in κ_ℓ . In comparison, in well known materials like silicon the inclusion of third or fourth nearest neighbors is quite adequate to obtain a satisfactorily converged thermal conductivity.²¹ Another factor is the large number of optical modes, as is common in systems with complex unit cells.²³ Optical phonons consistently account

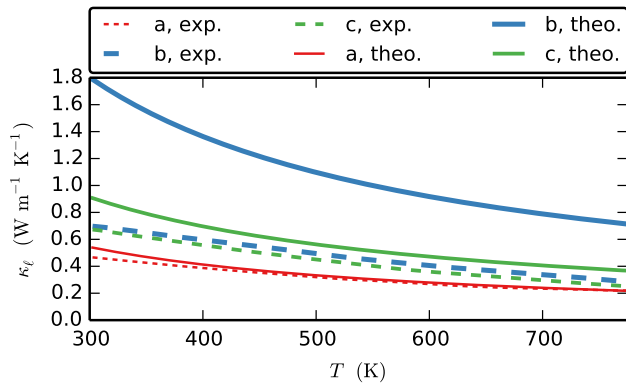


FIG. 3. Lattice thermal conductivity of the Pnma phase of SnSe: comparison between experimental results from Ref. 5 and theoretical computations in this letter.

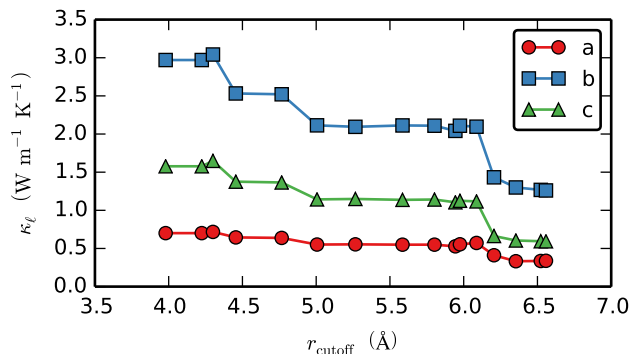


FIG. 4. Convergence of the lattice thermal conductivity of the Pnma phase of SnSe at $T = 500$ K with respect to the force cutoff employed in third-order calculations. Points represent actual calculations; lines are provided only as a guide to the eye.

for $\sim 45\%$ of κ_ℓ along a , and $\sim 65\%$ of its values along b or c . In-plane anisotropy is manifested in the fact that along c optical modes below and above the gap are almost on equal footing, whereas along b the lower-frequency group is responsible for more than 70% of the total optical contribution.

The polycrystalline character of a sample tends to shorten the phonon mean free paths (MFPs) below their intrinsic bulk values. To address the consistency of our monocrystalline results with experimental polycrystalline measurements, we must examine the MFPs of the phonons responsible for thermal transport. In Fig. 5 we show the reduction in κ_ℓ obtained by removing the contribution from all phonons with MFPs above a certain threshold, and at an intermediate temperature $T = 500$ K. All relevant MFPs lie below 100 nm. It is therefore relatively safe to compare the thermal conductivity of a single crystal to those of polycrystalline samples with grain sizes on the order of 10 to 100 μm , such as those recently reported.⁷

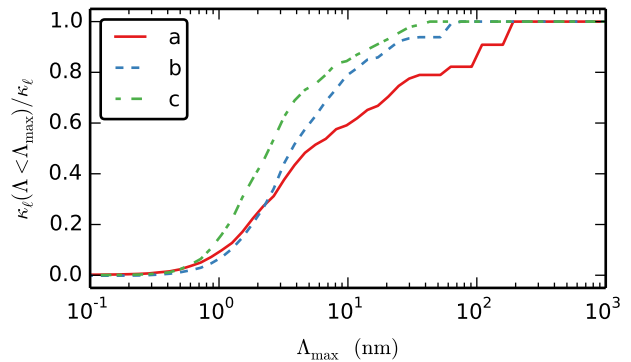


FIG. 5. Normalized cumulative lattice thermal conductivity of the Pnma phase of SnSe at $T = 500$ K.

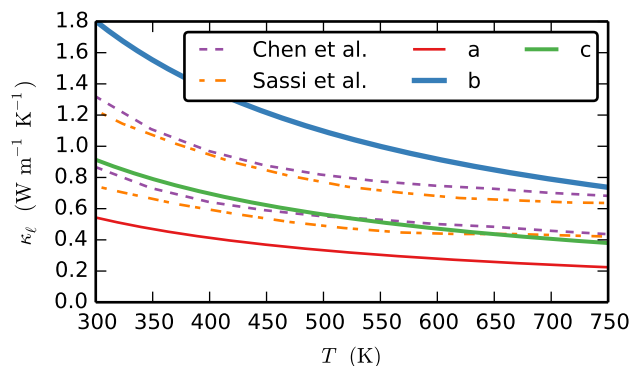


FIG. 6. Comparison of our result for single-crystal SnSe with recent results on polycrystals.^{6,7}

However, this comparison cannot be fully quantitative. One reason is due to our lack of a detailed description of grain boundaries in each particular experimental sample. More importantly, the methodology used in Refs. 6 and 7 cannot fully resolve the anisotropy of the material. Measurements are provided only along two directions: parallel and perpendicular to the pressing direction. Based on the experimental details and on x-ray powder diffraction patterns,⁶ perpendicular measurements are expected to represent a linear combination of κ_ℓ^b and κ_ℓ^c . Meanwhile, parallel measurements can include contributions from all three axes.

All things considered, the comparison between single-crystal theoretical calculations and the experimental results from polycrystals shown in Fig. 6 is satisfactory. More specifically, these results demand that at least one of the three principal values of the bulk thermal conductivity be significantly higher than any of those provided in Ref. 5. If the figure of merit reported in Ref. 5 is recalculated using the values of κ_ℓ reported in this letter while keeping the power factor constant, its values along b and c become lower and closer to that along a . This brings them more in line with the largely isotropic values measured in polycrystals.^{6,7}

In conclusion, we have used a fully *ab-initio* method to study the lattice thermal conductivity of the Pnma phase of SnSe over a broad temperature range. We were motivated by three different sets of experimental results. One was performed on monocrystalline samples,⁵ and the remaining two for polycrystals.^{6,7} The latter two studies seem to contradict the former, which would place SnSe as the best thermoelectric ever measured. Our results for the long axis of the SnSe structure agree with Ref. 5. Over the other two axes our calculations differ from those measurements in two crucial aspects. One of these is that the computed values of κ_{ℓ} , while still remarkably low, are higher than those measured. The other is that the two short axes are completely non-equivalent from a thermal transport viewpoint. In contrast, the limited amount of information about monocrystalline SnSe that can be extracted from the experiments on polycrystals^{6,7} seems to be fully compatible with our results, as are historical measurements on single crystals.⁸

Our calculations have allowed us to identify the *b* crystallographic direction as a facile axis for phonon flow. Our detailed study of the phonon frequencies, group velocities, and mean free paths help illuminate the structural foundations for such behavior. This is consistent with a thermoelectric figure of merit with a lower degree of anisotropy, as observed in polycrystals.^{6,7} The information provided by our study will hopefully be useful for designing improved nanoengineering approaches to further optimize this promising thermoelectric.

ACKNOWLEDGMENTS

The authors thank Dr. E. Alleno, Dr. G. Bernard-Granger, Dr. J. Heremans, Dr. B. Lenoir and Dr. A. Stelling for insightful discussion. This work is partially supported by the French “Carnot” project SIEVE, by DOD-ONR (N00014-13-1-0635, N00014-11-1-0136, N00014-09-1-0921). S. C. acknowledges partial support by DOE (DE-AC02-05CH11231), specifically the BES program under Grant #EDCBEE. The consortium

AFLOWLIB.org acknowledges Duke University—Center for Materials Genomics — and the CRAY corporation for computational assistance.

- ¹H. J. Goldsmid, *Introduction to Thermoelectricity* (Springer-Verlag, Berlin, 2009).
- ²S. Curtarolo, G. L. W. Hart, M. Buongiorno Nardelli, N. Mingo, S. Sanvito, and O. Levy, *Nat. Mater.* **12**, 191 (2013).
- ³A. J. Minnich, M. S. Dresselhaus, Z. F. Ren, and G. Chen, *Energy Environ. Sci.* **2**, 466 (2009).
- ⁴S. K. Bux, R. G. Blair, P. K. Gogna, H. Lee, G. Chen, M. S. Dresselhaus, R. B. Kaner, and J.-P. Fleurial, *Adv. Func. Mater.* **19**, 2445 (2009).
- ⁵L.-D. Zhao, S.-H. Lo, Y. Zhang, H. Sun, G. Tan, C. Uher, C. Wolverton, V. P. Dravid, and M. G. Kanatzidis, *Nature* **508**, 373 (2014).
- ⁶S. Sassi, C. Candolfi, J.-B. Vaney, V. Ohorodniichuk, P. Masschelein, A. Dauscher, , and B. Lenoir, *Appl. Phys. Lett.* **104**, 212105 (2014).
- ⁷C.-L. Chen, H. Wang, Y.-Y. Chen, T. Day, and J. Snyder, in press, *J. Mater. Chem. A* (2014), 10.1039/C4TA01643B.
- ⁸J. D. Wasscher, W. Albers, and C. Haas, *Solid-State Electron.* **6**, 261 (1963).
- ⁹D. A. Broido, M. Malorny, G. Birner, N. Mingo, and D. A. Stewart, *Appl. Phys. Lett.* **91**, 231922 (2007).
- ¹⁰A. Ward and D. A. Broido, *Phys. Rev. B* **81**, 085205 (2010).
- ¹¹X. Tang and J. Dong, *Proc. Natl. Acad. Sci. USA* **107**, 4539 (2010).
- ¹²W. Li and N. Mingo, *J. Appl. Phys.* **114**, 183505 (2013).
- ¹³L. Lindsay, W. Li, J. Carrete, N. Mingo, D. A. Broido, and T. L. Reinecke, *Phys. Rev. B* **89**, 155426 (2014).
- ¹⁴S. Curtarolo, W. Setyawan, S. Wang, J. Xue, K. Yang, R. H. Taylor, L. J. Nelson, G. L. W. Hart, S. Sanvito, M. Buongiorno Nardelli, N. Mingo, and O. Levy, *Comp. Mat. Sci.* **58**, 227 (2012).
- ¹⁵R. H. Taylor, F. Rose, C. Toher, O. Levy, K. Yang, M. Buongiorno Nardelli, and S. Curtarolo, in press, *Comp. Mat. Sci.* (2014), 10.1016/j.commatsci.2014.05.014.
- ¹⁶G. Kresse and J. Furthmüller, *Phys. Rev. B* **54**, 11169 (1996).
- ¹⁷J. P. Perdew and A. Zunger, *Phys. Rev. B* **23**, 5048 (1981).
- ¹⁸P. E. Blöchl, *Phys. Rev. B* **50**, 17953 (1994).
- ¹⁹T. Chattopadhyay, J. Pannetier, and H. V. Schnering, *J. Phys. Chem. Solids* **47**, 879 (1986).
- ²⁰A. Togo, F. Oba, and I. Tanaka, *Phys. Rev. B* **78**, 134106 (2008).
- ²¹W. Li, J. Carrete, N. A. Katcho, and N. Mingo, *Comp. Phys. Commun.* **185**, 17471758 (2014).
- ²²K. E. Goodson, *Science* **315**, 342 (2007).
- ²³G. A. Slack, in *Solid State Physics*, Vol. 34, edited by H. Ehrenreich, F. Seitz, and D. Turnbull (Academic, New York, 1979) p. 1.